



Published in final edited form as:

*EcoSal Plus*. 2018 August ; 8(1): . doi:10.1128/ecosalplus.ESP-0004-2018.

## An Introduction to the Structure and Function of the catalytic core enzyme of *Escherichia coli* RNA polymerase

Catherine Sutherland<sup>1</sup> and Katsuhiko S. Murakami<sup>1,2</sup>

<sup>1</sup>Department of Biochemistry and Molecular Biology, The Center for RNA Molecular Biology, The Pennsylvania State University, University Park, PA 16802

### Abstract

RNA polymerase (RNAP) is the essential enzyme responsible for transcribing the genetic information stored in DNA to RNA. Understanding the structure and function of RNAP is important for those who study basic principles in gene expression, such as the mechanisms of transcription and its regulation, as well as translational sciences such as antibiotic development. With over a half-century of investigations, there is a wealth of information available on the structure and function of *Escherichia coli* RNAP. This review introduces the structural features of *E. coli* RNAP, organized by subunit, giving information on the function, location, and conservation of these features to early stage investigators who have just started their research of *E. coli* RNAP.

### INTRODUCTION

The *Escherichia coli* RNA polymerase (RNAP) is a multi-subunit enzyme composed of five subunits including  $\alpha$  (two copies),  $\beta$ ,  $\beta'$  and  $\omega$  subunits. These five subunits form the RNAP core enzyme responsible for RNA synthesis using DNA as template and ribonucleotide (rNTP) as substrate. For initiating promoter specific DNA transcription, the core enzyme has to bind a  $\sigma$  factor, which helps to direct the polymerase to specific promoters. The core polymerase with sigma factor is referred to as the holoenzyme. Bacteria express several different forms of  $\sigma$  factor that are able to recognize and bind different promoter sequences in response to various signals and environmental conditions. *E. coli* expresses seven types of  $\sigma$  factor.  $\sigma^{70}$  belongs to the group 1  $\sigma$  factor, which is responsible for expressing housekeeping genes and has four independent domains (domains 1-4). Domain 4 recognizes the -35 element as double-stranded DNA form whereas domain 2 recognizes the -10 element as single-stranded DNA form. Other  $\sigma$  factors are for expressing genes for stress responses including group 3 ( $\sigma^{32}$ ,  $\sigma^{38}$ ), extracytoplasmic function (ECF) or group 4 ( $\sigma^E$ ,  $\sigma^I$ ) and RpoN ( $\sigma^{54}$ )  $\sigma$  factors (Feklistov et al., 2014; Riordan and Mitra, 2017).

Since the first discovery of RNAP in the early 1960s (Hurwitz, 2005), the *E. coli* RNAP has been the primary model system of choice for understanding functions of cellular RNAPs for many reasons. For example, the transcriptional activity of RNAP can be easily probed *in vitro* in the presence of purified template DNA and transcription factors. RNAP can be conveniently reconstituted *in vitro* from its individual subunits using either wild-type or

<sup>2</sup>Correspondence: kum14@psu.edu.

mutant proteins to probe their functions (Fujita and Ishihama, 1996). RNAP can be also prepared from co-overexpression systems (Artsimovitch et al., 2003), which can be used not only for biochemical assay but also for structural study of RNAP containing antibiotic resistance mutations (Molodtsov et al., 2017). A simple and robust *E. coli* transcription system also makes it an excellent model for single-molecule studies of RNAPs (Harada et al., 1999; Larson et al., 2011).

Structural study of *E. coli* RNAP began by using electron microscopy in the late-1980s (Darst et al., 1989). The near-atomic resolution X-ray crystal structure of *E. coli* RNAP was determined first as holoenzyme containing  $\sigma^{70}$  (Murakami, 2013). X-ray crystal and cryo-electron microscopy (cryo-EM) structures of *E. coli* RNAP are now available in several forms such as holoenzymes containing alternative  $\sigma$  factors (Liu et al., 2016; Yang et al., 2015), promoter DNA complexes (Glyde et al., 2017; Zuo and Steitz, 2015), elongation complex (Kang et al., 2017), in complex with transcription factors (Bae et al., 2013; Liu et al., 2017; Molodtsov et al., 2018), and with inhibitors/antibiotics (Bae et al., 2015; Chen et al., 2017; Degen et al., 2014; Molodtsov et al., 2015; Molodtsov et al., 2013), providing details of the structure and function of *E. coli* RNAP transcription and regulation.

### **$\alpha$ subunit**

The  $\alpha$  subunit (329 residues, 36.5 kDa in *E. coli*), encoded in the *rpoA* gene, is the second smallest subunit in the bacterial RNAP core enzyme and exists as a homodimer (Fig. 1B, Table 1). The  $\alpha$  subunit consists of two structural domains including the N-terminal ( $\alpha$ NTD, 1-235 residues) and C-terminal domains ( $\alpha$ CTD, 248-329 residues) (Fig. 2A). Both domains fold independently and are connected by a flexible linker (236-247 residues). The  $\alpha$ NTD can be further separated into two domains. Domain 1 (residues 1-52 and 180-235) consists of two alpha helices (H1 and H3) and a four-stranded antiparallel  $\beta$  sheet. Domain 2 (53-179) consists of 7 antiparallel  $\beta$  strands and one  $\alpha$  helix (H3). Only domain 1 is involved in  $\alpha$  dimerization. A key interaction during dimerization is the result of interlock between two pairs of  $\alpha$  helices (H1 and H3) from each  $\alpha$ NTD that form a hydrophobic core with highly conserved amino acid residues.

The primary function of the  $\alpha$  subunit is RNAP assembly. The formation of the  $\alpha$  dimer is the first step in RNAP biogenesis and it acts as a scaffold for assembling the two largest subunits  $\beta$  and  $\beta'$ . One of the  $\alpha$  subunits ( $\alpha$ 1) contacts only the  $\beta$  subunit (1,624 Å<sup>2</sup>) while the other  $\alpha$  subunit ( $\alpha$ 2) largely contacts the  $\beta'$  subunit (960 Å<sup>2</sup>) and also makes minor contacts with the  $\beta$  subunit (280 Å<sup>2</sup>). The  $\alpha$  dimer forms a complex with the  $\beta$  subunit but not  $\beta'$  subunit, indicating the assembly scheme of the bacterial RNAP follows as Fig. 1A.

Assembly with these large subunits occurs exclusively on one face of the  $\alpha$  dimer in two different places. The  $\beta$  subunit interacts with  $\alpha$ 1 subunit residues 45–48 and around residue 80, whereas the  $\beta'$  subunit interacts with  $\alpha$ 2 subunit around residue 80 and with residues 173–200. An  $\alpha$  derivative having an Arg45 to Ala substitution (R45A) retains  $\alpha$  dimerization and  $\beta'$  binding but cannot associate with the  $\beta$  subunit, making it possible to form hybrid RNAP containing two distinct  $\alpha$  subunit derivatives in a defined orientation (Murakami et al., 1997a).

An additional function of the  $\alpha$ NTD is the interaction with transcription factors for gene regulation. The classical transcription regulator in *E. coli*, catabolite activator protein (CAP), binds at  $-41.5$  base position relative to the transcription start site (+1) of the galactose operon promoter, and interacts with the  $\alpha$ NTD at four acidic residues (162-165) in a loop region of domain 2 of the  $\alpha$ NTD (Lawson et al., 2004).

The  $\alpha$ CTD is not essential for RNAP assembly and basal level transcription (Igarashi et al., 1991). However, it is important in transcription activation for interacting with multiple transcription factors and DNA. The  $\alpha$ CTD is the first domain of RNAP shown to directly interact with transcription factors (Igarashi and Ishihama, 1991) and to have its structure determined at high-resolution (Jeon et al., 1995). The function of the  $\alpha$ CTD for transcription regulation was discovered by chance. To define the minimal region of the  $\alpha$  subunit responsible for RNAP assembly, the  $\alpha$ CTD was deleted. The  $\alpha$ CTD deletion mutant showed the same level of transcription activity *in vitro* as the wild-type RNAP for transcription factor-independent promoters, however, the mutant did not demonstrate the CAP-dependent transcription activation at the lactose operon promoter (Igarashi and Ishihama, 1991) having the CAP binding site at  $-61.5$  base position relative to the transcription start site. After this discovery, the *E. coli* RNAP mutant lacking the  $\alpha$ CTD and the *in vitro* transcription system became important tools for hunting the transcription factors interacting with RNAP via the  $\alpha$ CTD and as a result many new factors were found (Ishihama, 1992). Locations of both copies of the  $\alpha$ CTD are dynamic, interacting with transcription factors at various positions on promoter DNA (Lee et al., 2012; Murakami et al., 1997b).

The  $\alpha$ CTD also interacts with an AT-rich DNA sequence, the UP element, found upstream of the  $-35$  element in strong *E. coli* promoters such as those for rRNAs (Ross et al., 1993). Amino acid residues that interact with transcription factors and DNA were mapped by site-directed mutagenesis of the  $\alpha$ CTD (Murakami et al., 1996) and the binding between the  $\alpha$ CTD and CAP as well as the  $\alpha$ CTD and UP element were revealed by the X-ray crystal and cryo-EM structures (Fig. 2B) (Benoff et al., 2002; Liu et al., 2017). The  $\alpha$ CTD establishes only weak interaction with DNA without direct contact with DNA bases; Arg265 of the  $\alpha$ CTD is a key amino acid residue for DNA interaction, which contacts the base pair edges with a hydrogen bond mediated by a water molecule.

### $\omega$ subunit

The  $\omega$  subunit (91 residues, 10.2 kDa in *E. coli*), encoded by the *rpoZ* gene, is the smallest subunit of bacterial RNAP (Fig. 1B, Table 1), and is the only subunit of RNAP dispensable for cell growth and for *in vitro* RNAP reconstitution with transcription activity (Gentry et al., 1991; Igarashi et al., 1989). Due to its non-essential role, its biological role has been studied minimally. Since the *rpoZ* strain of *E. coli* co-purifies RNAP with global protein chaperone GroEL (Mukherjee et al., 1999), one of the proposed functions of the  $\omega$  subunit is a chaperone for RNAP folding. The  $\omega$  subunit consists of five  $\alpha$  helices and binds mainly to the  $\beta'$  subunit (contact surface:  $1,348 \text{ \AA}^2$ ), particularly to the double-psi- $\beta$ -barrel (DPBB) domain (Fig. 3A). The DPBB domain of the  $\beta'$  subunit contains the active site for RNA synthesis, suggesting a role of  $\omega$  subunit in maintaining RNAP catalytic activity and/or protecting the DPBB domain against various damages.

It has been proposed that the  $\omega$  subunit plays a role in responding to the bacterial alarmone ppGpp, a global gene regulator, during the stringent response. The binding of ppGpp to  $\omega$  subunit (ppGpp binding site 1) was discovered by crosslinking experiments (Ross et al., 2013) and X-ray crystal structures of *E. coli* RNAP in complex with ppGpp (Mechold et al., 2013; Zuo et al., 2013). The N-terminal region of the  $\omega$  subunit together with the DPBB domain of the  $\beta'$  subunit are involved in the binding of ppGpp (Fig. 3B). The 5'- and 3'-phosphate groups face the R3 and R52 residues of the  $\omega$  subunit, respectively. The guanine base faces the  $\beta'$  subunit and His364/Asp622 residues form hydrogen bonds with the guanine base, explaining the specificity for guanine binding at the ppGpp binding site 1. Based on sequence conservation of the N-terminal region of  $\omega$  subunit, the ppGpp binding site 1 is likely conserved in not only the  $\gamma$ -proteobacteria such as *E. coli* but also in the  $\alpha$ - and  $\beta$ -proteobacteria (Hauryliuk et al., 2015). Recent studies identified another ppGpp binding site near the secondary channel of RNAP, which is  $\sim 60$  Å away from the site 1. The second ppGpp binding site is formed only in the presence of the RNAP binding transcription regulator DksA (Molodtsov et al., 2018; Ross et al., 2016).

### $\beta$ and $\beta'$ subunits

The  $\beta$  and  $\beta'$  subunits (1,342 and 1,407 residues), encoded in the *rpoB* and *rpoC* genes in the  $\beta$  operon, are the two largest subunits of RNAP with molecular weights of 150 and 155 kDa respectively (Fig. 1B, Table 1). Although the  $\beta$  and  $\beta'$  subunits form a complex with a large protein-protein interface ( $7,734$  Å<sup>2</sup>), their assembly still requires the  $\alpha$  dimer as their binding platform. The *rpoB* and *rpoC* genes are organized in an operon with *rpoB* positioned upstream of *rpoC*. Furthermore, in the 3D structure of RNAP, the C-terminus of  $\beta$  subunit is adjacent to the N-terminus of  $\beta'$  subunit, suggesting that these two subunits may have been fused together in the ancient form of cellular RNAP. In support of this hypothesis, an engineered  $\beta$  and  $\beta'$  subunit fusion still forms a functional RNAP (Severinov et al., 1997).

The  $\beta$  and  $\beta'$  subunits occupy 80 % of the total mass of core enzyme and form each claw arm of the crab claw shape of RNAP, generating a cleft for template DNA entry into the enzyme active site which is located at the bottom of the cleft (Fig. 4A). The active site is formed by two double-psi beta-barrel (DPBB) domains, one from each of the  $\beta$  and  $\beta'$  subunits. The DPBB of the  $\beta'$  subunit contains the aspartic acid triad in the sequence motif -DFDGD- for coordinating the catalytic Mg<sup>2+</sup> ions for the nucleotidyl transfer reaction. The DPBB domain of the  $\beta$  subunit has basic residues on its surface for interacting with the incoming nucleotide (Basu et al., 2014). All cellular RNAPs from bacteria to human use the DPBB domains for RNA synthesis. Nucleotide substrates enter into the active site of RNAP through the secondary channel, a funnel-shaped opening separate from the main channel by the bridge helix of  $\beta'$  subunit (Fig. 4A) (Zhang et al., 2015). The secondary channel acts as a binding cavity for accessory factors that modulate RNAP activity such as Gre factors (Opalka et al., 2003) and that regulate transcription such as DksA and TraR (Molodtsov et al., 2018). Two additional motifs from the  $\beta'$  subunit play important roles in the RNA synthesis reaction: the trigger loop for the catalysis and the bridge helix for the DNA/RNA translocation during the nucleotide addition cycle (Fig. 4B) (Mishanina et al., 2017).

In many crystal structures of RNAP, the trigger loop is disordered indicating that it is a highly mobile element. During catalysis, an incoming NTP enters via the secondary channel and the trigger loop begins to fold allowing the NTP to position at the pre-insertion site. Once the NTP correctly establishes a Watson-Crick base pair with the template DNA base, the trigger loop finishes folding into an  $\alpha$  helical hairpin structure causing the NTP to align with the catalytic  $Mg^{2+}$  and the 3' end of the RNA thus facilitating the nucleotidyl transfer reaction. After nucleotide addition, the trigger loop returns to an unfolded state, pyrophosphate is released, and the DNA/RNA hybrid is translocated to prepare for the next round of the reaction (Brueckner et al., 2009) (<https://www.youtube.com/watch?v=YZTsPeRDdeA>). Analogously, varying conformations of the bridge helix have been identified in various structures of RNAP indicating its dynamic role in the nucleotide addition cycle. The bridge helix folds into a helical bundle structure that facilitates the folding of the trigger loop thus helping to coordinate catalysis. The bridge helix is also believed to be important in translocation of RNAP as it cycles between straight and bent conformations (Cheung and Cramer, 2012; Silva et al., 2014; Svetlov and Nudler, 2009).

During transcription, RNAP unwinds double-stranded DNA to form the transcription bubble containing the single-stranded non-template DNA and the 8~9 bp template DNA and RNA hybrid. RNAP moves along DNA while maintaining the transcription bubble until the end of RNA synthesis. Four protein loops from the  $\beta$  and  $\beta'$  subunits including fork loop 2 and switch 3 of the  $\beta$  subunit as well as the lid and rudder of the  $\beta'$  subunit, form an interaction network with the DNA and RNA strands in the transcription bubble (Fig. 4B). The lid stacks on the upstream base pair and sterically blocks growth of the DNA/RNA hybrid in order for RNA to separate from the template DNA. The rudder interacts with DNA separated from the hybrid preventing re-association with the RNA. Switch 3 interacts with the first displaced RNA base presumably to help the separation of RNA from the hybrid and the re-annealing of the template and non-template DNA strands. Downstream DNA is accommodated at the cleft of the main channel and maintains its duplex DNA structure. Fork loop 2 plays a role in DNA strand separation as an Arg side chain stacks on the DNA base pair and blocks the passage of the duplex DNA towards the active site.

The  $\beta$  and  $\beta'$  subunits together form the DNA binding clamp, which changes its conformation during transcription. The clamp is open in apo-form RNAP and early intermediates in the RNAP and promoter DNA complex but closes upon formation of a stable open complex and remains closed during transcription elongation (Chakraborty et al., 2012; Feklistov et al., 2017). The main channel of RNAP is positively charged for DNA binding, however, the surface of RNAP is negatively charged for preventing non-specific interactions with DNA.

Another important domain of the  $\beta$  subunit is the flap domain, which covers the RNA exit pathway from the active site to outside of RNAP. During the nucleotide addition cycle, single stranded RNA passes underneath it to exit from RNAP. Transcription of palindromic DNA sequences causes RNA hairpins to form. RNA secondary structure formation within the narrow RNA exit pathway influences the conformation of the flap domain and then in turn causes transcription pausing and termination (Ray-Soni et al., 2016).

### Rifampicin binding pocket of the $\beta$ subunit

Bacterial RNAP is an excellent target for antimicrobial drugs (antibiotics). One of the most widely used antibiotics against bacterial RNAP is Rifampin (RMP), which is a member of the Rifamycin family of antibiotics for treating tuberculosis caused by the bacterium *Mycobacterium tuberculosis* (MTB) (Aristoff et al., 2010). RMP binds in the middle of the RNA extension pathway within the  $\beta$  subunit, therefore, it sterically blocks the elongation of the nascent RNA transcript. The RMP resistance mutations are located in amino acid residues 507-533 of the  $\beta$  subunit, the RMP resistance-determining region (RRDR) of *rpoB*. Mutations in the 81 bp of DNA encoding the RRDR are used as a marker for detecting multi-drug resistant TB (MDR-TB) (Fig. 4C). Although 90 non-synonymous *rpoB* mutations in the RRDR were found in clinical RMP resistance MTB isolates, around 85% of isolates involve the amino acid substitutions at Ser531 to Leu (S531L, 41%), His526 to Tyr (H526Y, 36%) and Asp516 to Val (D516V, 9%). The crystal structures of the *E. coli* RNAP including the RMP resistance mutants D516V, H526Y and S531L showed that each mutation elicits different structural and/or surface electrostatic potential changes which make the  $\beta$  subunit surface less favorable for binding RMP (Molodtsov et al., 2017).

### Lineage specific insertions in the $\beta$ and $\beta'$ subunit

The  $\beta$  and  $\beta'$  subunits are highly conserved throughout evolution. Nevertheless, large sequence insertions in  $\beta$  and  $\beta'$  characterize specific evolutionary lineages of bacteria (Lane and Darst, 2010). *E. coli*  $\beta$  and  $\beta'$  subunits have insertions in between the highly conserved regions (Fig. 1B). There are two insertions in the  $\beta$  subunit including  $\beta$  insertion 4 ( $\beta$ i4, residues 225–343) and  $\beta$  insertion 9 ( $\beta$ i9, residues 938–1042).  $\beta$ i4 is located at the tip of the lobe domain positioned at one of pincers of the double-stranded DNA binding cleft.  $\beta$ i9 is located in the middle of the flap domain. The  $\beta'$  subunit has one insertion,  $\beta'$  insertion 6 ( $\beta'$ i6, residues 942–1129) in the middle of the trigger loop, which plays an important role in all stages of transcription, including the stabilization of the open complex, transcription pausing, and termination (Artsimovitch et al., 2003).

### ACKNOWLEDGEMENTS

This work was supported by NIH grants GM087350 (K.S.M.).

### REFERENCES

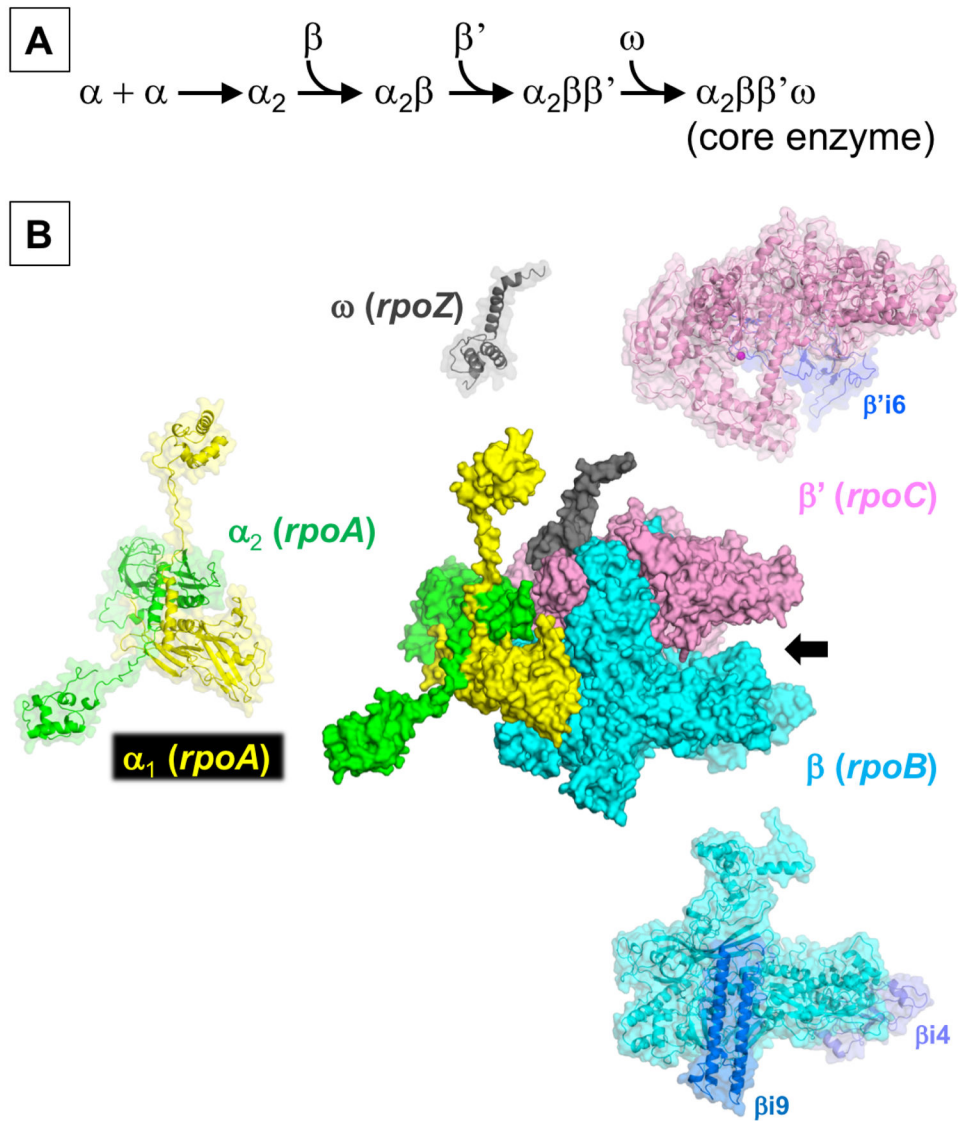
- Aristoff PA , Garcia GA , Kirchoff PD , and Showalter HD (2010). Rifamycins – Obstacles and Opportunities. *Tuberculosis* 90, 94–118. [PubMed: 20236863]
- Artsimovitch I , Svetlov V , Murakami KS , and Landick R (2003). Co-overexpression of Escherichia coli RNA polymerase subunits allows isolation and analysis of mutant enzymes lacking lineage-specific sequence insertions. *J Biol Chem* 278, 12344–12355. [PubMed: 12511572]
- Bae B , Davis E , Brown D , Campbell EA , Wigneshweraraj S , and Darst SA (2013). Phage T7 Gp2 inhibition of Escherichia coli RNA polymerase involves misappropriation of sigma70 domain 1.1. *Proc Natl Acad Sci U S A* 110, 19772–19777. [PubMed: 24218560]
- Bae B , Nayak D , Ray A , Mustaev A , Landick R , and Darst SA (2015). CBR antimicrobials inhibit RNA polymerase via at least two bridge-helix cap-mediated effects on nucleotide addition. *Proc Natl Acad Sci U S A* 112, E4178–4187. [PubMed: 26195788]

- Basu RS , Warner BA , Molodtsov V , Pupov D , Esyunina D , Fernandez-Tomero C , Kulbachinskiy A , and Murakami KS (2014). Structural basis of transcription initiation by bacterial RNA polymerase holoenzyme. *J Biol Chem* 289, 24549–24559. [PubMed: 24973216]
- Benoff B , Yang EL , Lawson CL , Parkinson G , Liu J , Blatter E , Ebright YW , Berman HM , and Ebright RH (2002). Structural basis of transcription activation: the CAP-alpha CTD-DNA complex. *Science* 297, 1562–1566. [PubMed: 12202833]
- Brueckner F , Ortiz J , and Cramer P (2009). A movie of the RNA polymerase nucleotide addition cycle. *Current opinion in structural biology* 19, 294–299. [PubMed: 19481445]
- Chakraborty A , Wang D , Ebright YW , Korlann Y , Kortkhonjia E , Kim T , Chowdhury S , Wigneshweraraj S , Irschik EL , Jansen R , et al. (2012). Opening and closing of the bacterial RNA polymerase clamp. *Science* 337, 591–595. [PubMed: 22859489]
- Chen J , Wassarman KM , Feng S , Leon K , Feklistov A , Winkelman JT , Li Z , Walz T , Campbell EA , and Darst SA (2017). 6S RNA Mimics B-Form DNA to Regulate Escherichia coli RNA Polymerase. *Molecular cell* 68, 388–397 e386. [PubMed: 28988932]
- Cheung AC , and Cramer P (2012). A movie of RNA polymerase II transcription. *Cell* 149, 1431–1437. [PubMed: 22726432]
- Darst SA , Kubalek EW , and Kornberg RD (1989). Three-dimensional structure of Escherichia coli RNA polymerase holoenzyme determined by electron crystallography. *Nature* 340, 730–732. [PubMed: 2671751]
- Degen D , Feng Y , Zhang Y , Ebright KY , Ebright YW , Gigliotti M , Vahedian-Movahed EL , Mandal S , Talaue M , Connell N , et al. (2014). Transcription inhibition by the depsipeptide antibiotic salinamide A. *Elife* 3, e02451. [PubMed: 24843001]
- Feklistov A , Bae B , Hauver J , Lass-Napiorkowska A , Kalesse M , Glaus F , Altmann KH , Heyduk T , Landick R , and Darst SA (2017). RNA polymerase motions during promoter melting. *Science* 356, 863–866. [PubMed: 28546214]
- Feklistov A , Sharon BD , Darst SA , and Gross CA (2014). Bacterial sigma factors: a historical, structural, and genomic perspective. *Annu Rev Microbiol* 68, 357–376. [PubMed: 25002089]
- Fujita N , and Ishihama A (1996). Reconstitution of RNA polymerase. *Methods Enzymol* 273, 121–130. [PubMed: 8791604]
- Gentry D , Xiao H , Burgess R , and Cashel M (1991). The omega subunit of Escherichia coli K-12 RNA polymerase is not required for stringent RNA control in vivo. *Journal of bacteriology* 173, 3901–3903. [PubMed: 1711031]
- Glyde R , Ye F , Darbari VC , Zhang N , Buck M , and Zhang X (2017). Structures of RNA Polymerase Closed and Intermediate Complexes Reveal Mechanisms of DNA Opening and Transcription Initiation. *Molecular cell* 67, 106–116 e104. [PubMed: 28579332]
- Harada Y , Funatsu T , Murakami K , Nonoyama Y , Ishihama A , and Yanagida T (1999). Single-molecule imaging of RNA polymerase-DNA interactions in real time. *Biophys J* 76, 709–715. [PubMed: 9929475]
- Haurlyuk V , Atkinson GC , Murakami KS , Tenson T , and Gerdes K (2015). Recent functional insights into the role of (p)ppGpp in bacterial physiology. *Nat Rev Microbiol* 13, 298–309. [PubMed: 25853779]
- Hurwitz J (2005). The discovery of RNA polymerase. *J Biol Chem* 280, 42477–42485. [PubMed: 16230341]
- Igarashi K , Fujita N , and Ishihama A (1989). Promoter selectivity of Escherichia coli RNA polymerase: omega factor is responsible for the ppGpp sensitivity. *Nucleic acids research* 17, 8755–8765. [PubMed: 2685748]
- Igarashi K , Fujita N , and Ishihama A (1991). Identification of a subunit assembly domain in the alpha subunit of Escherichia coli RNA polymerase. *J Mol Biol* 218, 1–6. [PubMed: 2002495]
- Igarashi K , and Ishihama A (1991). Bipartite functional map of the E. coli RNA polymerase alpha subunit: involvement of the C-terminal region in transcription activation by cAMP-CRP. *Cell* 65, 1015–1022. [PubMed: 1646077]
- Ishihama A (1992). Role of the RNA polymerase alpha subunit in transcription activation. *Mol Microbiol* 6, 3283–3288. [PubMed: 1484484]

- Jeon YH , Negishi T , Shirakawa M , Yamazaki T , Fujita N , Ishihama A , and Kyogoku Y (1995). Solution structure of the activator contact domain of the RNA polymerase alpha subunit. *Science* 270, 1495–1497. [PubMed: 7491496]
- Kang JY , Olinares PD , Chen J , Campbell EA , Mustaev A , Chait BT , Gottesman ME , and Darst SA (2017). Structural basis of transcription arrest by coliphage HK022 N<sub>un</sub> in an Escherichia coli RNA polymerase elongation complex. *Elife* 6.
- Lane WJ , and Darst SA (2010). Molecular evolution of multisubunit RNA polymerases: sequence analysis. *J Mol Biol* 395, 671–685. [PubMed: 19895820]
- Larson MH , Landick R , and Block SM (2011). Single-molecule studies of RNA polymerase: one singular sensation, every little step it takes. *Molecular cell* 41, 249–262. [PubMed: 21292158]
- Lawson CL , Swigon D , Murakami KS , Darst SA , Berman HM , and Ebright RH (2004). Catabolite activator protein: DNA binding and transcription activation. *Current opinion in structural biology* 14, 10–20. [PubMed: 15102444]
- Lee DJ , Minchin SD , and Busby SJ (2012). Activating transcription in bacteria. *Annu Rev Microbiol* 66, 125–152. [PubMed: 22726217]
- Liu B , Hong C , Huang RK , Yu Z , and Steitz TA (2017). Structural basis of bacterial transcription activation. *Science* 358, 947–951. [PubMed: 29146813]
- Liu B , Zuo Y , and Steitz TA (2016). Structures of E. coli sigmaS-transcription initiation complexes provide new insights into polymerase mechanism. *Proc Natl Acad Sci U S A* 113, 4051–4056. [PubMed: 27035955]
- Mechold U , Potrykus K , Murphy H , Murakami KS , and Cashel M (2013). Differential regulation by ppGpp versus pppGpp in Escherichia coli. *Nucleic acids research* 41, 6175–6189. [PubMed: 23620295]
- Mishanina TV , Palo MZ , Nayak D , Mooney RA , and Landick R (2017). Trigger loop of RNA polymerase is a positional, not acid-base, catalyst for both transcription and proofreading. *Proc Natl Acad Sci U S A* 114, E5103–E5112. [PubMed: 28607053]
- Molodtsov V , Fleming PR , Eyermann CJ , Ferguson AD , Foulk MA , McKinney DC , Masse CE , Burman ET , and Murakami KS (2015). X-ray crystal structures of Escherichia coli RNA polymerase with switch region binding inhibitors enable rational design of squaramides with an improved fraction unbound to human plasma protein. *J Med Chem* 58, 3156–3171. [PubMed: 25798859]
- Molodtsov V , Nawarathne IN , Scharf NT , Kirchhoff PD , Showalter HD , Garcia GA , and Murakami KS (2013). X-ray crystal structures of the Escherichia coli RNA polymerase in complex with benzoxazinorifamycins. *J Med Chem* 56, 4758–4763. [PubMed: 23679862]
- Molodtsov V , Scharf NT , Stefan MA , Garcia GA , and Murakami KS (2017). Structural basis for rifamycin resistance of bacterial RNA polymerase by the three most clinically important RpoB mutations found in Mycobacterium tuberculosis. *Mol Microbiol* 103, 1034–1045. [PubMed: 28009073]
- Molodtsov V , Sineva E , Zhang L , Huang X , Cashel M , Ades SE , and Murakami KS (2018). Allosteric effector ppGpp potentiates the inhibition of transcript initiation by DksA. *Molecular cell*.
- Mukherjee K , Nagai H , Shimamoto N , and Chatterji D (1999). GroEL is involved in activation of Escherichia coli RNA polymerase devoid of the omega subunit in vivo. *Eur J Biochem* 266, 228–235. [PubMed: 10542069]
- Murakami K , Fujita N , and Ishihama A (1996). Transcription factor recognition surface on the RNA polymerase alpha subunit is involved in contact with the DNA enhancer element. *EMBO J* 15, 4358–4367. [PubMed: 8861963]
- Murakami K , Kimura M , Owens JT , Meares CF , and Ishihama A (1997a). The two alpha subunits of Escherichia coli RNA polymerase are asymmetrically arranged and contact different halves of the DNA upstream element. *Proc Natl Acad Sci U S A* 94, 1709–1714. [PubMed: 9050843]
- Murakami K , Owens JT , Belyaeva TA , Meares CF , Busby SJ , and Ishihama A (1997b). Positioning of two alpha subunit carboxy-terminal domains of RNA polymerase at promoters by two transcription factors. *Proc Natl Acad Sci U S A* 94, 11274–11278. [PubMed: 9326599]



- Murakami KS (2013). X-ray crystal structure of *Escherichia coli* RNA polymerase sigma70 holoenzyme. *J Biol Chem* 288, 9126–9134. [PubMed: 23389035]
- Opalka N , Chlenov M , Chacon P , Rice WJ , Wriggers W , and Darst SA (2003). Structure and function of the transcription elongation factor GreB bound to bacterial RNA polymerase. *Cell* 114, 335–345. [PubMed: 12914698]
- Ray-Soni A , Bellecourt MJ , and Landick R (2016). Mechanisms of Bacterial Transcription Termination: All Good Things Must End. *Annu Rev Biochem* 85, 319–347. [PubMed: 27023849]
- Riordan JT , and Mitra A (2017). Regulation of *Escherichia coli* Pathogenesis by Alternative Sigma Factor N. *EcoSal Plus* 7.
- Ross W , Gosink KK , Salomon J , Igarashi K , Zou C , Ishihama A , Severinov K , and Gourse RL (1993). A third recognition element in bacterial promoters: DNA binding by the alpha subunit of RNA polymerase. *Science* 262, 1407–1413. [PubMed: 8248780]
- Ross W , Sanchez-Vazquez P , Chen AY , Lee JH , Burgos HL , and Gourse RL (2016). ppGpp Binding to a Site at the RNAP-DksA Interface Accounts for Its Dramatic Effects on Transcription Initiation during the Stringent Response. *Molecular cell* 62, 811–823. [PubMed: 27237053]
- Ross W , Vrentas CE , Sanchez-Vazquez P , Gaal T , and Gourse RL (2013). The magic spot: a ppGpp binding site on *E. coli* RNA polymerase responsible for regulation of transcription initiation. *Molecular cell* 50, 420–429. [PubMed: 23623682]
- Severinov K , Mooney R , Darst SA , and Landick R (1997). Tethering of the large subunits of *Escherichia coli* RNA polymerase. *J Biol Chem* 272, 24137–24140. [PubMed: 9305860]
- Silva DA , Weiss DR , Pardo Avila F , Da LT , Levitt M , Wang D , and Huang X (2014). Millisecond dynamics of RNA polymerase II translocation at atomic resolution. *Proc Natl Acad Sci U S A* 111, 7665–7670. [PubMed: 24753580]
- Svetlov V , and Nudler E (2009). Macromolecular micromovements: how RNA polymerase translocates. *Current opinion in structural biology* 19, 701–707. [PubMed: 19889534]
- Yang Y , Darbari VC , Zhang N , Lu D , Glyde R , Wang YP , Winkelman JT , Gourse RL , Murakami KS , Buck M , et al. (2015). TRANSCRIPTION. Structures of the RNA polymerase-sigma54 reveal new and conserved regulatory strategies. *Science* 349, 882–885. [PubMed: 26293966]
- Zhang L , Silva DA , Pardo-Avila F , Wang D , and Huang X (2015). Structural Model of RNA Polymerase II Elongation Complex with Complete Transcription Bubble Reveals NTP Entry Routes. *PLoS Comput Biol* 11, e1004354. [PubMed: 26134169]
- Zuo Y , and Steitz TA (2015). Crystal structures of the *E. coli* transcription initiation complexes with a complete bubble. *Molecular cell* 58, 534–540. [PubMed: 25866247]
- Zuo Y , Wang Y , and Steitz TA (2013). The mechanism of *E. coli* RNA polymerase regulation by ppGpp is suggested by the structure of their complex. *Molecular cell* 50, 430–436. [PubMed: 23623685]

**Figure 1.**

**A)** Assembly scheme of the RNAP core enzyme. **B)** Structural overview of the *E. coli* RNAP core enzyme shown as a molecular surface representation ( $\alpha_1$ : yellow,  $\alpha_2$ : green,  $\beta$ : cyan,  $\beta'$ : pink, and  $\omega$ : gray) (PDB: 4YG2). The DNA binding main channel is indicated by a black arrow. Individual subunits are also depicted with partially transparent surface to expose the ribbon model inside. Lineage specific insertions found in the  $\beta$  ( $\beta i4$  and  $\beta i9$ ) and  $\beta'$  subunits ( $\beta' i6$ ) are indicated in blue. The active site is represented by the catalytic  $Mg^{2+}$  ion (magenta sphere) coordinated in the  $\beta'$  subunit.

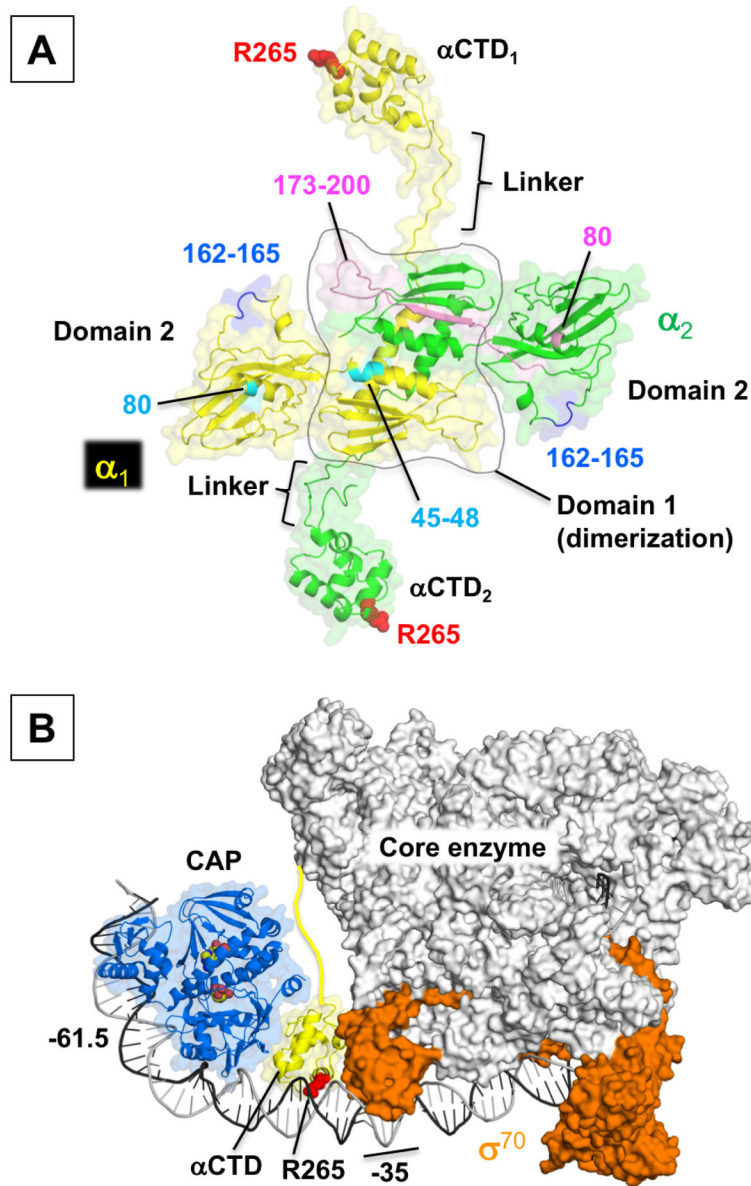


**Figure 2.**

**A)** Dimerization of  $\alpha$  subunits ( $\alpha_1$ : yellow,  $\alpha_2$ : green). Structural domains and linkers for connecting the  $\alpha$ NTD and  $\alpha$ CTD are indicated. Amino acid residues contacting with the  $\beta$  and the  $\beta'$  are highlighted in cyan and pink, respectively. Amino acid residues of  $\alpha$ NTD responsible for the interaction with CAP are highlighted in blue. Arg265 in the  $\alpha$ CTD for the UP element DNA interaction is shown in red color CPK representation. **B)** Structural model of the CAP (light blue), RNAP (core enzyme, white;  $\sigma^{70}$ , orange) and *lac* promoter DNA complex (PDB: 6B6H). The CAP binds DNA centered at position  $-61.5$  relative to the transcription start site (+1) and interacts with one copy of the  $\alpha$ CTD positioning between the CAP and  $\sigma^{70}$ . A linker (236-247 residues) connecting between the NTD and CTD of  $\alpha$  subunit is shown as yellow line.

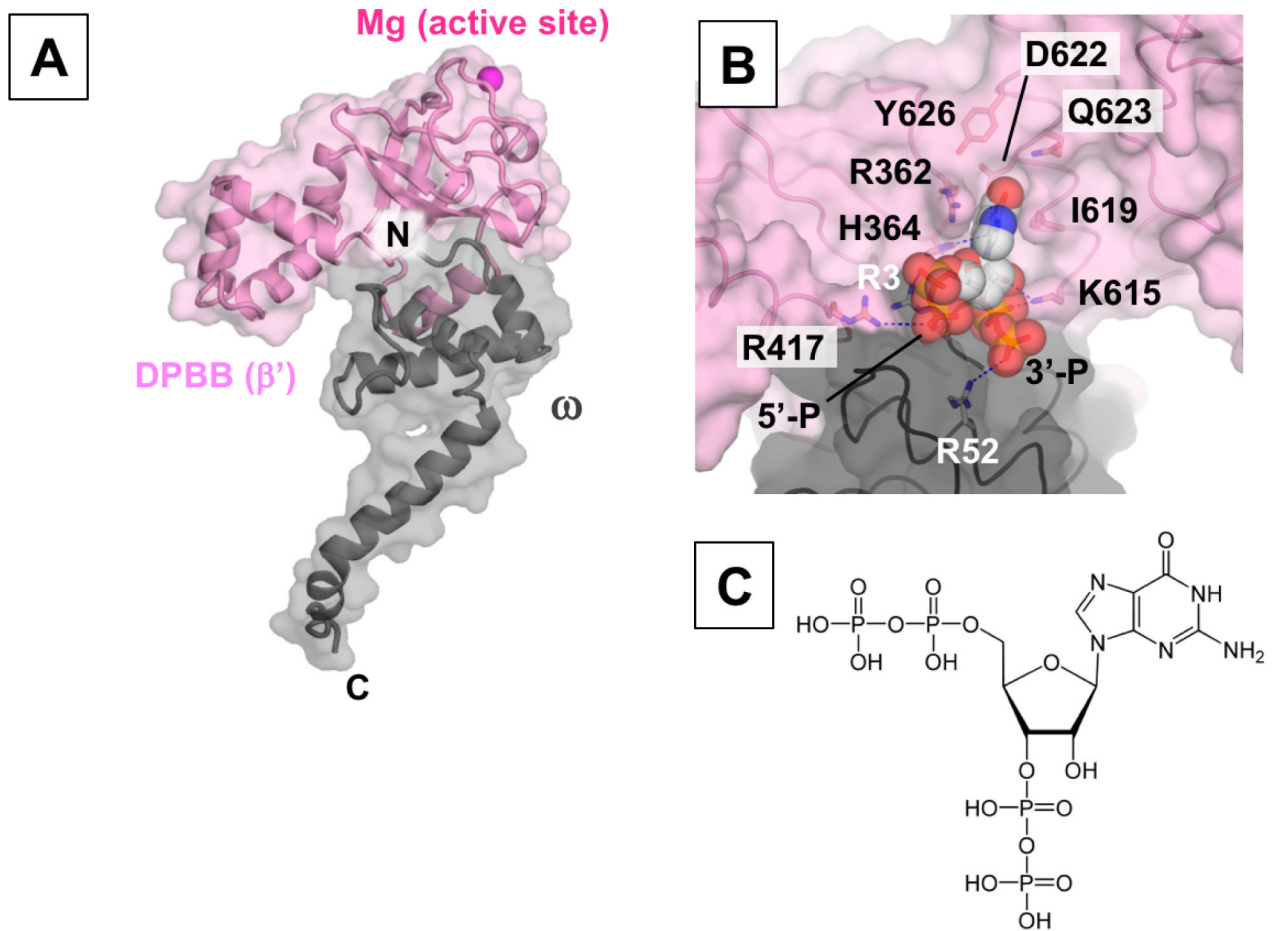


**Figure 3.**

**A)** Interaction between the  $\omega$  subunit and the DPBB domain of  $\beta'$  subunit. The  $Mg^{2+}$  coordinated at the active site of RNAP is shown as a magenta sphere. **B)** The ppGpp site 1 ( $\omega$ , gray;  $\beta'$ , pink and ppGpp, CPK model). Amino acid residues that interact with ppGpp are shown as stick models and indicated.

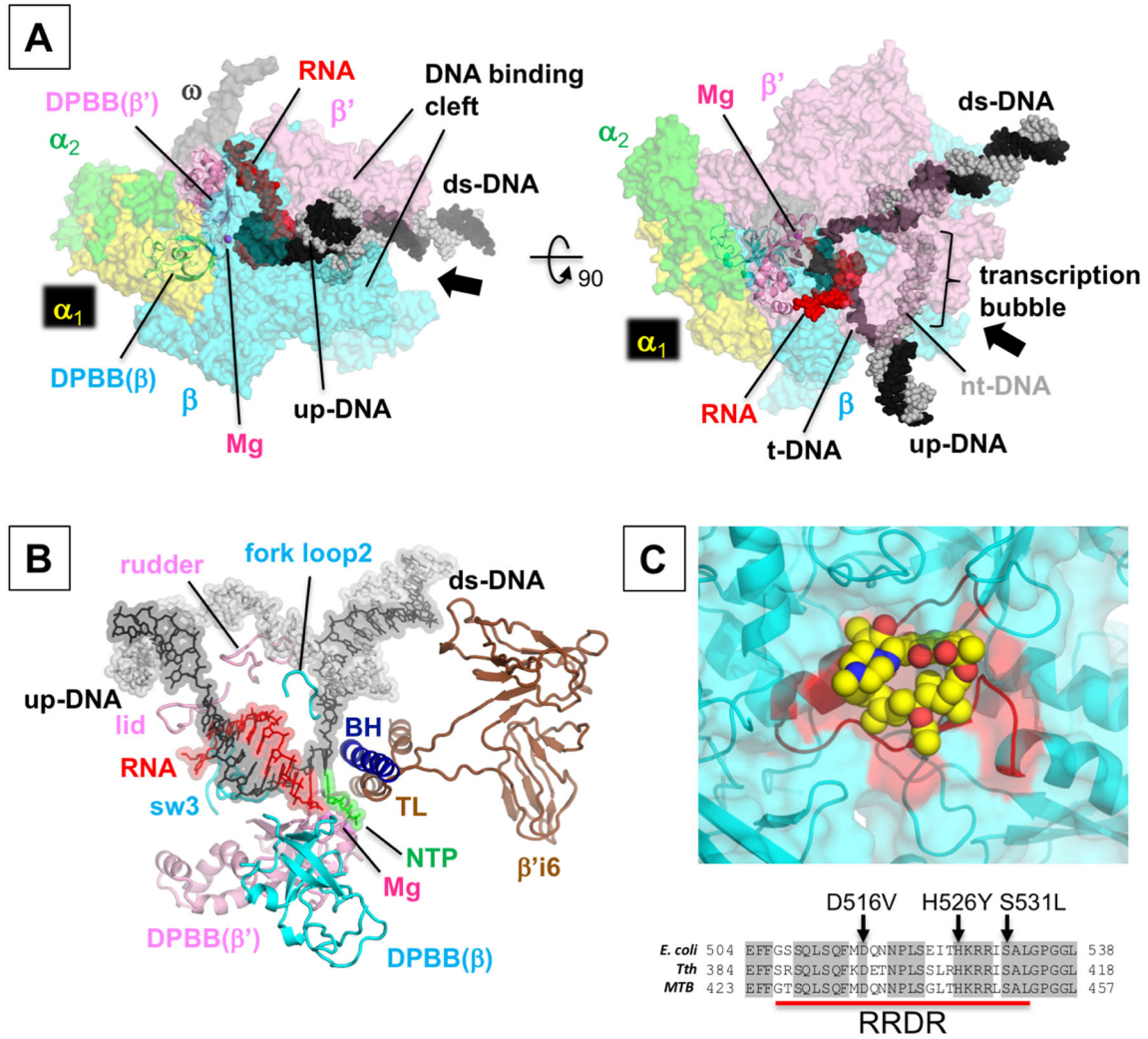


**Figure 4.**  
**A)** Structural model of the *E. coli* RNAP elongation complex (PDB: 6ALF with modification). The core enzyme is depicted as partially transparent surface model with the DPBB domains of  $\beta$  and  $\beta'$  subunits (ribbon models). DNA and RNA are shown as CPK models (RNA, red; template DNA, black; non-template DNA, light gray). The DNA binding main channel is indicated by a black arrow. **B)** Important structural features of the active site (BH, bridge helix; TL, trigger loop). **C)** (top) Rifampin binding pocket of the  $\beta$  subunit (Rifampin, CPK model;  $\beta$  subunit, partially transparent surface with ribbon model). Amino acid residues in the RRDR are highlighted in red. (bottom) Sequence alignment spanning RRDRs of the *E. coli*, *T. thermophilus* and MTB RNAP. Amino acids that are identical among the three species are shown as gray background. Three most clinically important RMP resistance mutations are indicated.

**Table 1.**Summary of subunits found in the *E. coli* RNAP core enzyme

Subunit (gene)	Size (MW)	Functions
$\alpha$ ( <i>rpoA</i> )	329 aa (36.5 kDa)	RNAP assembly (NTD), interactions with DNA and transcription factors for transcriptional regulation
$\beta$ ( <i>rpoB</i> )	1342 aa (150.4 kDa)	DNA and RNA binding, RNA synthesis, NTP binding, RMP binding site, $\sigma$ factor binding
$\beta'$ ( <i>rpoC</i> )	1407 aa (155.0 kDa)	DNA binding, RNA synthesis, catalytic $Mg^{2+}$ coordination, ppGpp binding site 1, $\sigma$ factor binding
$\omega$ ( <i>rpoZ</i> )	91 aa (10.2 kDa)	RNAP folding, ppGpp binding site 1

Author Manuscript

Author Manuscript

Author Manuscript

Author Manuscript